Non-local phonon thermal conductivity

Philip B. Allen*
Department of Physics and Astronomy, Stony Brook University, Stony Brook, New York 11794-3800, USA
(Dated: December 4, 2016)

In insulating crystals, the long phonon mean-free path enhances the non-locality of the relation $\kappa(x-x')$ between a steady state heat current $\vec{J}(x)$ and the temperature gradient $\vec{\nabla}T(x')$. In Fourier space, $j(q) = -\kappa(q)\nabla T(q)$. Inevitable non-locality complicates the understanding of nanoscale heat-transfer. Non-local information is now becoming measurable by modern sub-micron imaging methods. A particular example, derived from simulations on crystalline GaN, is analyzed. The results provide a trove of new information. Simplified formulas are derived to assist the analysis.

I. INTRODUCTION

The long mean free paths of small-Q acoustic phonons causes the local temperature $T(x)$ to depend on distant heat sources, as seen in Fig. 1. Such non-local effects are increasingly important because of miniaturization of heat-generating electronics, and because of development of temperature probes with improving spatial resolution. But even in the simplest case of a homogeneous crystal, the non-local relation $\kappa(x-x')$ between heat current $j(x)$ and temperature gradient $-\nabla T(x')$ is extremely interesting, although mostly neglected. This paper shows some ways of studying and trying to understand it. In the homogeneous case, linear response implies the relation

$$j(x) = -\int dx' \kappa(x-x')\nabla_{x'}T(x') \;\rightarrow\; j(q) = -\kappa(q)\nabla T(q). \tag{1}$$

This assumes that spatial variation occurs only in the x-direction. The range $|x-x'|$ is at least as long as the mean free path $|\vec{v}_Q|\tau_Q$ (where $\vec{v}_Q = \vec{\nabla}_Q\omega_Q$) of the phonons ω_Q which carry significant amounts of heat.

Figure 1 is derived from a simulation by Zhou *et al.*[1] for a periodically repeated segment of GaN. This simulation applied heat $H(x)$ uniformly in chosen slabs and removed it from others, as illustrated later in Fig. 5a. Numerical integration of Newton's laws gave classical trajectories of all 60,000 atoms. The classical picture is sufficient since $\hbar\omega/k_B \leq 300$K for the most important heat-carrying vibrational modes. After steady state is reached, the spatially-varying temperature is found at a grid of locations by averaging for several ps. This method is called "non-equilibrium molecular dynamics" (NEMD). The forces driving the atoms are taken from a phenomenological interatomic force law of imperfect accuracy. Nevertheless, the realism is impressive and appropriate for further analysis. However, the numerical result, a value $\kappa_{\rm eff} \sim 90$W/mK, derived from the ratio of the known heat flux to the computed mid-point temperature gradient, has definitely not converged to the bulk answer κ, as explained by Zhou *et al.*[1]. An aim of the present paper is to offer some explanation, and insight about extrapolation to the bulk limit.

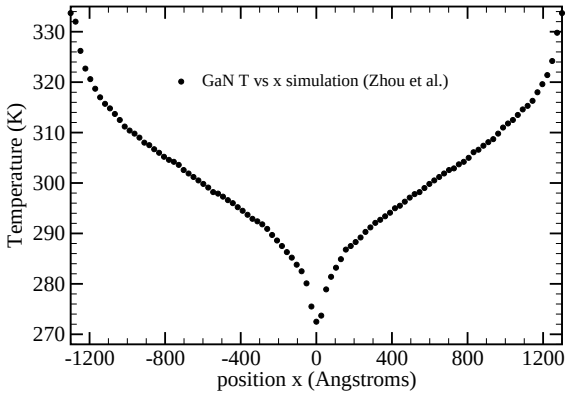

FIG. 1. Wurtzite-structure GaN simulated by Zhou *et al.*[1]. A segment of length $\Delta x = L = 500c = 2600\mathring{A}$ (along the c-axis) and cross section $A = 15\sqrt{3}a^2 = 264\mathring{A}^2$, containing 60,000 atoms, was periodically repeated. The average temperature was fixed at T =301.2K. Heat $H = 0.03$eV/ps$\mathring{A}^2$ was added to segments of width $12c$ at $-L/2$ (and equivalently at $+L/2$) and extracted at $L = 0$. The temperature plotted here was digitized from Fig. 6d of Ref. 1, where it had been averaged for each of 100 segments of width $5c$. The gradient $dT/dx = 0.0265\text{K}/\mathring{A}$ was found at midpoints $\pm L/4$ corresponding to $\kappa_{\rm eff}$ =90.43W/mK. The true bulk limit κ is higher by an unknown amount.

II. FOURIER TRANSFORMS

The information in Fig.1 is Fourier transformed following Ref.2. The resulting values of $\kappa(q)$ are shown in Fig.2. The wavevector q has only N possible values $q_n = 2\pi n/L$ for $-N/2+1 \leq n \leq N/2$, where $L/N = w$ is the width of the separate segments where T is averaged. But there are only $N/4$ independent real numbers in the $T(x)$ data shown, since $T(-x)$ converges to the same value as $T(x)$, and $T(L/4+x)-\bar{T}$ converges to the same value as $-T(L/4-x)+\bar{T}$ (barring small non-linear effects). Therefore there are only $N/4 = 25$ real numbers in the Fourier representation, which can be taken as the values of $\kappa(q_n)$ for positive odd integers n. Even integers n do not contribute because of the $T(-x) = T(x)$ symmetry. Only the smallest 12 q_n's are shown in Fig. 2. Higher q_n's are increasingly noisy. Partly this is caused by noise in the original calculations, and partly by addi-

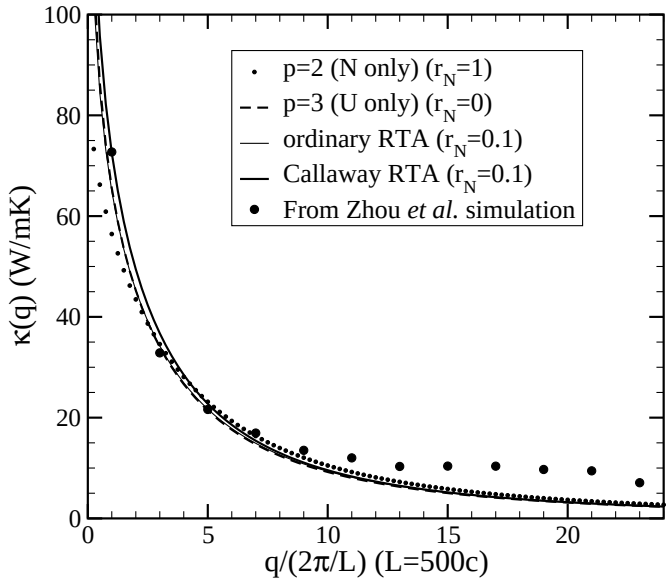

FIG. 2. The non-local $\kappa(q)$ is constructed for GaN at 300K, by Fourier transforming the $T(x)$ results shown in Fig. 1. The same two adjustable parameters (κ_0 =30.3 W/mK and $\ell_{\rm min} = 40c/\pi = 66\mathring{A}$) are used in all four theoretical curves. These are discussed in the text. The "Callaway RTA" curve is presumed closest to reality.

tional noise in the digitization (original numerical information was not available.)

III. BOLTZMANN $\kappa(q)$

GaN is a very good thermal conductor, because its phonons have long mean free paths. Thus it is a good "phonon gas" and should be accurately treated by the Peierls[3] Boltzmann equation. Using N_Q to designate the steady-state, non-equilibrium, phonon distribution function, and Ω to represent the volume of the crystal, the equations are

$$j(x) = \frac{1}{\Omega}\sum_Q \hbar\omega_Q v_{Qx} N_Q(x);$$

$$j(q) = \frac{1}{\Omega}\sum_Q \hbar\omega_Q v_{Qx} N_Q(q);$$

$$\left(\frac{dN_Q}{dt}\right)_{\rm drift} + \left(\frac{dN_Q}{dt}\right)_{\rm scatt} = 0. \qquad (2)$$

The distribution function N_Q can be separated into a "local equilbrium" part $n_Q = n_Q(T(x))$, (or $n_Q(T(q))$ in Fourier space), and the deviation Φ_Q. Here n_Q is the Bose-Einstein function, which becomes $k_BT/\hbar\omega_Q$ in the classical limit. The "drift" term in Eq.(2) then has the form $-v_{Qx}(dn_Q/dT)\nabla T(q) - iqv_{Qx}\Phi_Q(q)$. The "scattering" term is complicated, but for a simple analysis at room temperature it is quite safe to use the "relaxation time approximation" (RTA), namely $-\Phi_Q(q)/\tau_Q$, where $1/\tau_Q$ is the relaxation rate of mode Q. The resulting Boltzmann (B) equation has the (B-RTA) solution,

$$\kappa(q) = \frac{k_B}{\Omega}\sum_Q \frac{v_{Qx}^2}{1/\tau_Q + iqv_{Qx}}. \qquad (3)$$

Here the classical approximation has been made, $\hbar\omega_Q dn_Q/dT \to k_B$.

IV. DEBYE $\kappa(q)$

Eq.(3) is known to reproduce quite well the true solution, if $1/\tau_Q$ is the actual complicated phonon relaxation rate. For qualitative understanding, simpler model are desirable. In the Debye model there are three acoustic phonon branches, all having the form $\omega_Q = v|\vec{Q}|$, all with the same velocity v. As a supplement to the Debye model, take the relaxation rates $1/\tau_Q$ to be $(1/\tau_D)(Q/Q_D)^p$. Here Q_D is the Debye wavevector, and $1/\tau_D$ is a maximum scattering rate, which depends on T, being linear in T at higher T. The scale of $\kappa(T)$ in the Debye model is

$$\kappa_0 = \frac{k_B v^2 \tau_D}{V_{\rm cell}} \qquad (4)$$

Then in Debye approximation, the B-RTA Eq.(3) becomes the BD-RTA result,

$$\kappa_D(q) = \frac{3k_Bv^2}{2V_{\rm cell}}\int_0^{Q_D}\frac{dQQ^2}{Q_D^3}\int_{-1}^{1}\frac{\mu^2 d\mu}{1/\tau_Q + iqv\mu} \qquad (5)$$

where μ is $\cos\theta$, and θ is the angle between the velocity (parallel to $\vec{Q}$) and the direction of the temperature gradient (parallel to $\vec{q} = q\hat{x}$).

There is no complete consensus about what the power p should be. Herring[4] advocated $p = 2$, but subsequent studies[5–7] differ. Most often, for Normal ($\vec{q}$-conserving) scattering, $p = 2$, while for Umklapp scattering ($\vec{Q}$ changing by a reciprocal lattice vector $\vec{G}$), $p = 3$. For general p, Eq.(5) becomes

$$\kappa_p(q) = \frac{3\kappa_0}{2}\int_0^1 dx\int_{-1}^1 d\mu\frac{x^2\mu^2}{x^p + i\lambda\mu} \qquad (6)$$

where $x = Q/Q_D$ and $\lambda = qv\tau_D = q\ell_{\rm min}$. Algebraic formulas are given elsewhere[8]. The answers simplify at large wavevector $q\ell_{\rm min} >> 1$,

$$\kappa_p(q) \to \frac{9\kappa_0}{(3+p)(q\ell_{\rm min})^2}. \qquad (7)$$

However, the Boltzmann equation should not be taken very seriously[9] unless the wavevector q is significantly

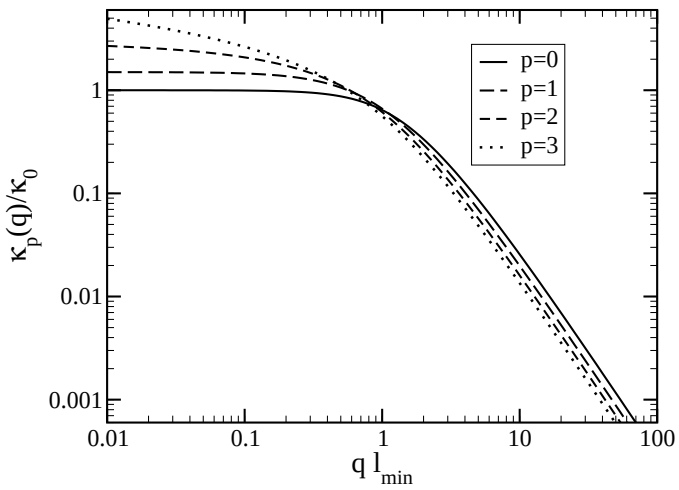

FIG. 3. Simple power law theories ($1/\tau_Q \propto Q^p$) from Boltzmann theory in RTA and Debye models. The $p = 2$ and 3 versions are shown in linear scale in Fig. 2.

smaller than the zone boundary π/a. The small-q part of the formulas is

$$\begin{aligned}
(p=0)\quad & \kappa_0(q) \sim \kappa_0(1 - 3\lambda^2/5 + \ldots) \\
(p=1)\quad & \kappa_1(q) \sim \frac{3}{2}\kappa_0 \left(1 - \frac{6}{5}\lambda^2 \log\frac{1}{\lambda} + \ldots\right) \\
(p=2)\quad & \kappa_2(q) \sim 3\kappa_0 \left(1 - \frac{3\pi}{7}\sqrt{\frac{\lambda}{2}} + \ldots\right) \\
(p=3)\quad & \kappa_3(q) \sim \kappa_0 \left(\log\frac{1}{\lambda} + \ldots\right)
\end{aligned} \tag{8}$$

Notice that the small-q parts for $p = 1, 2$ have non-analytic q-dependences, and the $p = 3$ formula diverges logarithmically. Full results (Eq. 6) are in Fig. 3.

V. CALLAWAY $\kappa(q)$

Callaway[10] devised an improved version of the relaxation time approximation. Anharmonic phonon interactions in good crystals conserve momentum *modulo* a reciprocal lattice vector $\vec{G}$. A phonon $\vec{Q}$ can decay into two phonons $\vec{Q}_1 + \vec{Q}_2$ provided $\vec{Q} = \vec{Q}_1 + \vec{Q}_2 + \vec{G}$. The N processes have $\vec{G} = 0$, and the U processes have $\vec{G} \neq 0$. Peierls[3] pointed out that N processes cannot fully relax the heat current. This is particularly important at lower T, because U processes require higher energy phonons and are thus suppressed at lower T.

Callaway's model for the rate of change of the phonon distribution N_Q is

$$\left(\frac{dN_Q}{dt}\right)_{\text{collision}} = -\frac{N_Q - n_Q}{\tau_{QU}} - \frac{N_Q - n^*_Q}{\tau_{QN}} \tag{9}$$

The distribution n^*_Q is the one which maximizes entropy subject to conservation of both energy and wavevector. It is a modified Bose-Einstein distribution

$$n^*_Q = \frac{1}{\exp(\hbar\omega_Q/k_BT + \Lambda_x Q_x) - 1}, \tag{10}$$

where Λ_x is a Lagrange multiplier fixed by the condition[11,12] $\sum_Q Q_x n^*_Q = Q_{x,\text{tot}} = \sum_Q Q_x \Phi_Q$. The natural extension of Debye-type relaxation laws in the Callaway scheme is

$$\begin{aligned}
1/\tau_{Q,\text{tot}} &= 1/\tau_{QU} + 1/\tau_{QN} = (1/\tau_D)(r_U x^3 + r_N x^2) \\
1/\tau_{QU} &= 1/\tau_U (Q/Q_D)^3 = (1/\tau_D) r_U x^3 \\
1/\tau_{QN} &= 1/\tau_N (Q/Q_D)^2 = (1/\tau_D) r_N x^2
\end{aligned} \tag{11}$$

where r_U and r_N are the relative rates of U and N scattering, with $r_U + r_N = 1$. The coefficients r_U and r_N depend strongly on T at low T, but are T-independent at higher T (where $1/\tau_D \propto T$). Zhou *et al.*[7] computed relaxation rates for GaAs in the classical limit. Their results (Fig. 2) indicate that $r_U \sim 0.9$ and $r_N \sim 0.1$. It is sensible to try the same values for GaN. Fig. 2 shows four versions of the BD-RTA theory. Two are single power-law forms with $p = 2$ or 3. One of them uses $1/\tau_{Q,\text{tot}}$ from Eq.(11), and the version of greatest realism uses the full Callaway RTA, Eq.(9).

VI. EXTRAPOLATING κ TO $L \to \infty$

Zhou *et al.*[1] attempt extrapolation of their finite size (L) simulations to $L \to \infty$, and note the difficulties encountered. The present results require alternate extrapolations. One way is to choose a model relaxation time and use the resulting BD-RTA theory to fit the $\kappa(q)$ curves in Fig. 2. Three things should be stressed. First, none of the theoretical curves fits the higher q part of $\kappa(q)$. This is not surprising. The theories describe small Q phonon properties, but do not recognize the small group velocities and corresponding small mean free paths of optical modes. These modes do carry heat, and are not suppressed at larger q. Second, a surprisingly nice fit with no theory at all can be made by plotting $\log\kappa(q)$ *versus* $\log q$. This is shown in Fig. 4. The observation that $\kappa(q)$ is proportional to $q^{-0.75}$ should not be taken seriously, even though it is a better fit than any obtained from BD-RTA theory. A $q^{-0.75}$ divergence implies a scaling $\kappa_{\text{bulk}} \propto L^{0.75}$ which would have been detected experimentally. Nevertheless, it is an intriguing observation which might motivate further investigation of behavior of $\kappa(q)$ in vibrational heat conductors. The third thing to be stressed is that fitting the $\kappa(q)$ data is an imperfect enterprise. The numerical $T(x)$ data of Zhou *et al.* shown in Fig. 1 were not originally intended for this purpose. The q-points for which numbers can be found are too sparse for fits with any care, and affected by noise both of computation and of the current digitization.

Nevertheless, theory does say things relevant here. All four fits shown in Fig. 2 provide ways of understanding the unexpectedly fast increase of $\kappa(q)$ as q decreases.

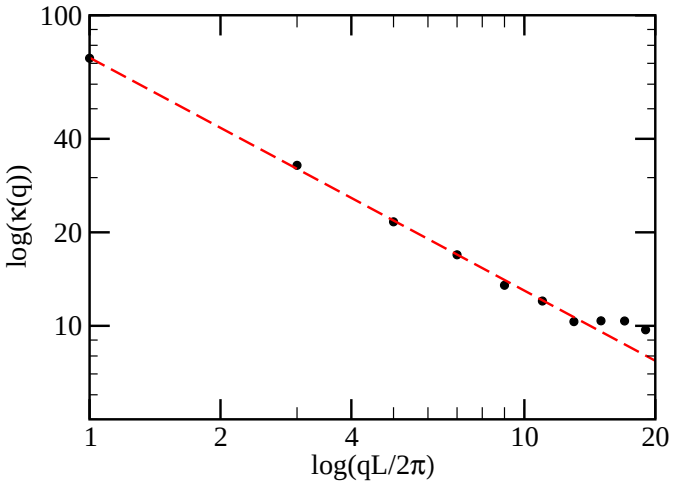

FIG. 4. The $\kappa(q)$ data from Fig. 2 are plotted here on a logarithmic scale, showing an approximate $\kappa \propto 1/q^{0.75}$ fit. This diverges strongly as $q \to 0$; the significance of this fit is unclear.

They also provide two kinds of guidance for extrapolation. First there is direct use of theory and numerics for $\kappa(q)$. The four curves in Fig. 2, when extended to $q = 0$, yield

$$
\begin{aligned}
&(p=2)\quad \kappa(0) = 3\kappa_0 \sim 91 \text{ W/mK} \\
&(p=3)\quad \kappa(0) = \infty \times \kappa_0 \sim \infty \\
&(\text{RTA},\ r_N = 0.1)\quad \kappa(0) = \frac{3\kappa_0}{r_U}\log\left(\frac{1}{r_N}\right) \\
&\qquad = 7.7\kappa_0 \sim 233 \text{ W/mK} \\
&(\text{Callaway})\quad \kappa(0) = \frac{\kappa_{\text{RTA}}}{1 - \frac{3r_N}{2r_U} + 3\left(\frac{r_N}{r_U}\right)^2 - 3\left(\frac{r_N}{r_U}\right)^3 \ln\left(\frac{1}{r_N}\right)} \\
&\qquad = \kappa_{\text{RTA}}/0.86 = 8.9\kappa_0 \sim 271 \text{ W/mK} \qquad (12)
\end{aligned}
$$

Evidently extrapolation to $L \to \infty$ is even more uncertain than imagined by Zhou *et al.*.

The other version of extrapolation indicated by this analysis is, following Zhou *et al.*, to plot κ_{eff} obtained from the temperature slope at mid-point, against various functions of L. Zhou *et al.* used $1/L$. Formulas derived here show that $1/\sqrt{L}$ has more theoretical justification and is in better correspondence with the $\kappa(q)$.

Finally, Fig. 5 suggests alternate ways of performing NEMD simulations. A more rapid reduction of noise will happen if instead of insertion of heat into discrete separated slabs (panel a), the heat is inserted sinusoidally (panel b). This has been tested[8] with some success for a simple model. But this gives only a single q-point for $\kappa(q)$, while a mesh of small-q points contains much additional insight. The heating pattern could use more than one sinusoidal periodicity, as in Fig. 5d. Finally, it is frustrating that the analysis done here yields only q_n with odd integer n; if $n = 2, 4, 6$ were available to supplement $n = 1, 3, 5$, then theoretical fits could be judged with far more confidence. The even integers were excluded by the mirror symmetry of the heat input. For example, the mirror in panel (a) is around $x = 0$, and in panel (b), around $x = L/4$. Arrangements like those shown in panels (c) and (d) provide the desired symmetry breaking.

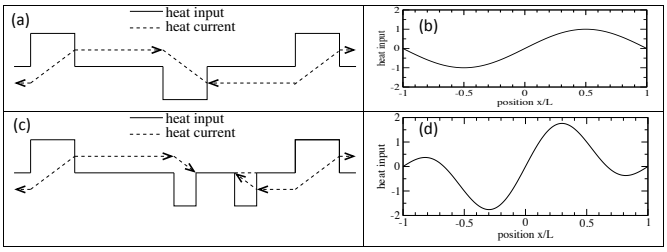

FIG. 5. Choice (a) is standard and used in Fig. 1. The others are suggested alternative heating profiles The sine curve (b) is the simplest. The asymmetrical block heating (c) allows all Fourier components to be extracted. Two sines (curve (d)) allows $q = 2\pi/L$ and $4\pi/L$ to be extracted simultaneously.

VII. ACKNOWLEDGEMENTS

This work was supported in part by DOE grant No. DE-FG02-08ER46550.

* philip.allen@stonybrook.edu

1. X. W. Zhou, S. Aubry, R. E. Jones, A. Greenstein, and P. K. Schelling, Phys. Rev. B **79**, 115201 (2009), URL http://link.aps.org/doi/10.1103/PhysRevB.79.115201.
2. P. B. Allen, Phys. Rev. B **90**, 054301 (2014), URL http://link.aps.org/doi/10.1103/PhysRevB.90.054301.
3. R. E. Peierls, Ann. Phys. **395**, 1055 (1929), URL http://dx.doi.org/10.1002/andp.19293950803.
4. C. Herring, Phys. Rev. **95**, 954 (1954).
5. K. Esfarjani, G. Chen, and H. T. Stokes, Phys. Rev. B **84**, 085204 (2011), URL http://link.aps.org/doi/10.1103/PhysRevB.84.085204.
6. J. Ma, W. Li, and X. Luo, Phys. Rev. B **90**, 035203 (2014), URL http://link.aps.org/doi/10.1103/PhysRevB.90.035203.
7. J. Zhou, B. Liao, and G. Chen, Semicond. Science and Tech. **31**, 043001 (2016).
8. Y. Li and P. B. Allen, arXiv1412.3099 (2014).
9. Note1, in metals, a corresponding Boltzmann equation gives a good theory for susceptibility $\chi(q,\omega)$ at small q and ω, but does not contain Friedel oscillations at $q = 2k_F$ or high frequency plasma oscillations or interband effects. For phonons, there is no analog of either Friedel or plasma

oscillations, so breakdown at large q, ω is probably gradual.
[10] J. Callaway, Phys. Rev. **113**, 1046 (1959), URL http://link.aps.org/doi/10.1103/PhysRev.113.1046.
[11] P. B. Allen, Phys. Rev. B **88**, 144302 (2013), URL http://link.aps.org/doi/10.1103/PhysRevB.88.144302.
[12] Note2, callaway used a slightly different and less correct condition.